PROCEEDINGS OF SCIENCE

LHCf Run II physics results in proton-proton collisions at $\sqrt{s}$ = 13 TeV

A. Tiberio,[a,*] **O. Adriani,**[a,b] **E. Berti,**[a,b] **P. Betti,**[a,b] **L. Bonechi,**[a] **M. Bongi,**[a,b] **R. D'Alessandro,**[a,b] **S. Detti,**[a] **M. Haguenauer,**[c] **Y. Itow,**[d,e] **K. Kasahara,**[f] **Y. Kitagami,**[d] **M. Kondo,**[d] **Y. Matsubara,**[d] **H. Menjo,**[d] **Y. Muraki,**[d] **K. Ohashi,**[d] **P. Papini,**[a] **G. Piparo,**[g,h] **S. Ricciarini,**[a,i] **T. Sako,**[j] **N. Sakurai,**[k] **M. Scaringella,**[a] **Y. Shimizu,**[l] **T. Tamura,**[l] **S. Torii,**[m] **A. Tricomi,**[g,h,n] **W. C. Turner**[o] **and K. Yoshida**[f]

[a] *INFN Section of Florence, Florence, Italy*
[b] *University of Florence, Florence, Italy*
[c] *Ecole-Polytechnique, Palaiseau, France*
[d] *Institute for Space-Earth Environmental Research, Furo-cho, Chikusa-ku, Nagoya, Japan*
[e] *Kobayashi-Maskawa Institute for the Origin of Particles and the Universe, Nagoya, Japan*
[f] *Faculty of System Engineering, Shibaura Institute of Technology, Tokyo, Japan*
[g] *INFN Section of Catania, Catania, Italy*
[h] *University of Catania, Catania, Italy*
[i] *IFAC-CNR, Florence, Italy*
[j] *Institute for Cosmic Ray Research, University of Tokyo, Chiba, Japan*
[k] *Tokushima University, Tokushima, Japan*
[l] *Kanagawa University, Kanagawa, Japan*
[m] *RISE, Waseda University, Shinjuku, Tokyo, Japan*
[n] *CSFNSM, Catania, Italy*
[o] *LBNL, Berkeley, California, USA*

E-mail: alessio.tiberio@fi.infn.it

PoS(ICHEP2022)121

*Speaker

The LHC-forward experiment (LHCf), located at the Large Hadron Collider (LHC), is designed to measure the production cross section of neutral particles in the very-forward region, covering the pseudorapidity region above 8.4 (up to zero-degree particles). By measuring the very-forward particle production rates at the highest energy possible at an accelerator, LHCf will provide fundamental informations to improve phenomenological hadronic interaction models used in the simulation of air-showers induced by ultra-high-energy cosmic rays in the atmosphere. The experiment consists of two small independent detectors placed 140 metres away from the ATLAS interaction point (IP1), on opposite sides. Each detector is made of two sampling and position sensitive calorimeters. This contribution will focus on the Run II physics results of LHCf in proton-proton collisions at 13 TeV. At first the photon energy spectrum will be presented and compared with the predictions of several hadronic interaction models. The advantages of the ATLAS-LHCf combined analysis will then be discussed and the preliminary spectrum of very-forward photons produced in diffractive collisions (tagged by ATLAS) will be shown together with models predictions. The preliminary Feynman-x and transverse momentum spectrum of π^0, and the Feynman-x spectrum of η will also be presented. Photons and π^0 production cross section provides important information about the electromagnetic component of an air-shower, while η measurements give the possibility to probe the strange-quark related contribution. Finally, the neutron energy spectrum measured in several pseudorapidity regions will be shown and compared with the predictions of various hadronic interaction models. From these measurements the average inelasticity of the collisions, which strongly affects the development of an air-shower, has also been extracted.

41st International Conference on High Energy physics - ICHEP2022
6-13 July, 2022
Bologna, Italy

1. Introduction

The indirect detection techniques of the Ultra-High-Energy Cosmic Rays (UHECRs) are based on the observation of the shower of secondary particles produced in the interaction of a cosmic ray with a nucleus of the atmosphere (the so-called "air-showers"). A clear interpretation of the data of ground based experiments is made difficult due to the large systematic uncertainty associated to the disagreement between different hadronic interaction models employed in the simulations of the air-showers. The tuning of these phenomenological models with experimental data is therefore fundamental to reduce the systematic uncertainty of UHECR measurements. The LHC-forward experiment (LHCf) is designed to measure the very-forward neutral particles production at the Large Hadron Collider (LHC). The very-forward region covered by LHCf is crucial for the tuning of hadronic interaction models since it is the region where most of the energy flow of secondary particles is contained. After a brief description of the experimental apparatus in Section 2, the LHCf analysis results for photon, neutron, π^0 and η production in proton-proton collisions at $\sqrt{s}$ = 13 TeV will be presented in Section 3.

2. The LHCf experiment

The LHCf experiment is composed of two independent detectors (named "Arm1" and "Arm2") placed ~140 meters away from the Interaction Point 1 [1]. The detectors are able to measure neutral particles emitted at a pseudorapidity $\gtrsim 8.4$, up to zero-degree. Each detector is made of two sampling and position sensitive calorimeters (called "towers" hereafter) which use Gd_2SiO_5 (GSO) scintillators as active layers and tungsten as absorber. Their energy resolution is better than 3% for photons above 100 GeV [2] and ~40% for neutrons. Each tower contains 4 couples of position sensitive layers to measure the transverse position: GSO scintillator bars are used in Arm1 while silicon microstrip detectors are used in Arm2. The position resolution for photons is 200μm and 40μm for Arm1 and Arm2 [2, 3], respectively, while the position resolution for neutrons is ~1 mm for both detectors.

3. LHCf physics results in p-p collisions at $\sqrt{s}$ = 13 TeV

The data set used in the following analyses has been collected during the low-luminosity LHCf dedicated run in proton-proton collisions at $\sqrt{s}$ = 13 TeV in LHC fill #3855. The photon and neutron analysis results shown in Section 3.1 and 3.4 used an integrated luminosity of 0.19 nb^{-1}. Type-I π^0 and η analyses used a larger data sample of 2.1 nb^{-1}, while Type-II π^0 analysis used a data sample of 0.8 nb^{-1} (see Section 3.2 for the explanation of the Type-I/II event categories).

3.1 Neutron energy spectrum and average inelasticity

The neutron energy spectrum in six pseudorapidity bins is shown in Figure 1 [4]. As previously noted [5], there is a significant disagreement between LHCf data and the predictions of the hadronic interaction models in the most forward region ($\eta > 10.75$): the peak structure of the data is not reproduced by any model and all models underestimate the neutron yield by at least 20%. In the other pseudorapidity regions either SIBYLL or EPOS models have a better agreement with respect to other models. The distribution of the elasticity of the collision ($k_n \equiv 2E_n/\sqrt{s}$, where E_n is the energy of the neutron) is shown in the top panel of Figure 2, while the average inelasticity $(1 - k_n)$ is shown in the bottom panel [4]. The average inelasticity predicted by all models is in good agreement with the measured one. However, k_n distribution is not well reproduced by any model.

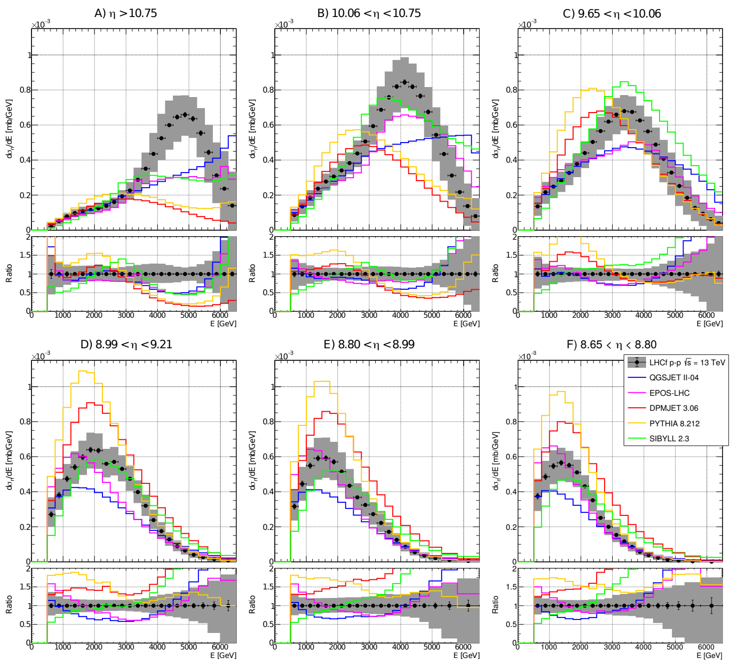

Figure 1: Measured neutron energy spectrum (black points) in different pesudorapidity bins compared with models predictions (coloured histograms). Grey area represents statistical+systematic uncertainty.

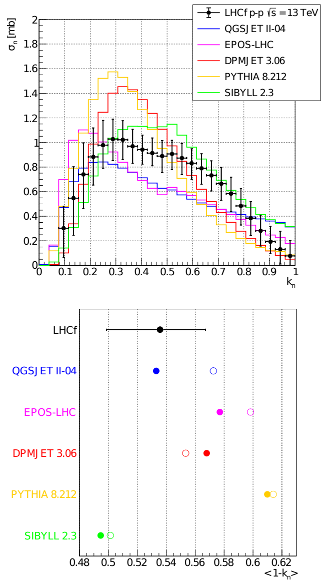

Figure 2: Top: neutron elasticity distribution for data (black points) and models predictions (coloured histograms). Bottom: average inelasticity for neutron events (full circles) and all event (open circles).

3.2 Neutral pion p_T vs X_F spectrum

The π^0 transverse momentum (p_T) and Feynman-X ($X_F \equiv 2p_Z/\sqrt{s}$) are reconstructed from the energy and impact position of the decay photons into the LHCf towers. Two typologies of events can be recorded: "Type I" events where one photon hits each tower, and "Type II" events where both photons hit the same tower. The preliminary p_T spectra in several X_F bins are shown in Figure 3. Type I and Type II analyses provide results in good agreement in the regions where they overlap, and Arm1 and Arm2 data also appear to be consistent with each other. The consistency of the data between different detectors and event types permits to fully take advantage of the different p_T and X_F coverage of Arm1 and Arm2, and of Type I and Type II events: Arm1 extends the highest measured p_T, while Arm2 covers (or reduces) the gaps in acceptance at p_T ~0.4÷0.5 GeV.

3.3 η meson X_F spectrum

The measurements of η production is an important probe for the dependency of the hadronic interaction models on the strange quark contribution, which is a key parameter of the models. η

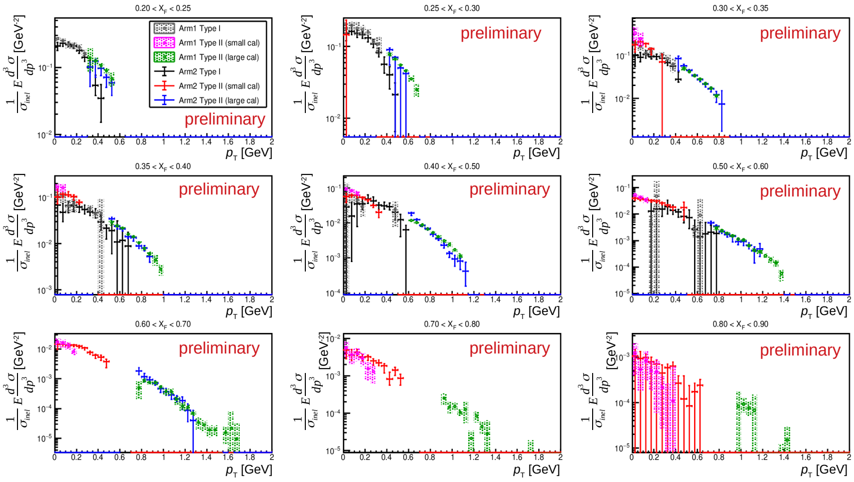

Figure 3: Transverse momentum spectra in different X_F bins measured with the Arm1 and Arm2 detectors of LHCf. Results from different detectors and π^0 event types are shown with different colors. Errors bars represent the total estimated uncertainty (statistical + systematic).

mesons are reconstructed in the same way as Type I π^0s. The reconstructed η invariant mass distribution and Feynman-X spectrum in the $P_T < 1.1$ GeV transverse momentum region obtained with the Arm2 detector are shown in Figure 4. QGSJET model shows a good agreement in the high-X_F region, but predicts a factor 2 lower yield at low energies. Other models exhibit a harder spectrum and a higher yield with respect to data.

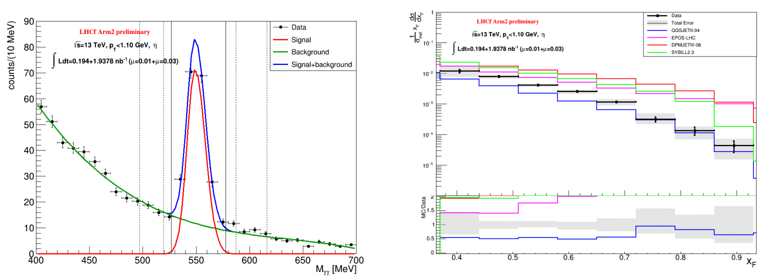

Figure 4: *Left:* η invariant mass distribution in the $P_T < 1.1$ GeV region reconstructed with the LHCf Arm2 detector. *Right:* X_F spectrum measured with the LHCf Arm2 detector compared with hadronic interaction models predictions. The shaded area represents the estimated total uncertainty.

3.4 LHCf-ATLAS combined photon analysis

LHCf and ATLAS experiments had a joint operation during all LHCf dedicated runs of Run II in order to be able to perform a combined analysis of the acquired data [6]. The number of tracks recorded by ATLAS detectors in the central region has been used to discriminate diffractive events from non-diffractive ones [7]. The preliminary results of the combined analysis are presented in Figure 5 , where the photon energy spectrum is shown for both the inclusive [8] and the low-mass diffraction component [6]. The diffraction spectrum of EPOS model has a good agreement with data in the $\eta > 10.94$ region, while PYTHIA model has a better agreement for $8.81 < \eta < 8.99$.

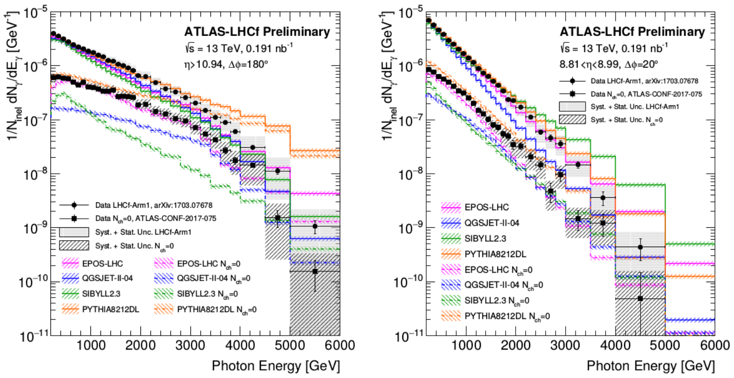

Figure 5: Photon energy spectrum for pseudorapidity regions $\eta > 10.94$ (left) and $8.81 < \eta < 8.99$ (right). Measured inclusive and low-mass diffractive spectra are represented as black circles and squares, respectively. Predictions from several hadronic interaction models for the inclusive and diffractive spectra are represented as solid and dashed lines, respectively. Hatched areas show total error for data and statistical error for models.

References

[1] O. Adriani et al., *The LHCf detector at the CERN large hadron collider*, *Journal of Instrumentation* **3** (2008) S08006.

[2] Y. Makino et al., *Performance study for the photon measurements of the upgraded LHCf calorimeters with Gd_2SiO_5 (GSO) scintillators*, *Journal of Instrumentation* **12** (2017) P03023.

[3] O. Adriani et al., *The construction and testing of the silicon position sensitive modules for the LHCf experiment at CERN*, *Journal of Instrumentation* **5** (2010) P01012.

[4] O. Adriani et al., *Measurement of energy flow, cross section and average inelasticity of forward neutrons produced in $\sqrt{s}$ = 13 TeV proton-proton collisions with the LHCf Arm2 detector*, *Journal of High Energy Physics* **2020** (2020) 16.

[5] O. Adriani et al., *Measurement of inclusive forward neutron production cross section in proton-proton collisions at $\sqrt{s}$ = 13 TeV with the LHCf Arm2 detector*, *Journal of High Energy Physics* **2018** (2018) 73.

[6] ATLAS and LHCf Collaborations, *Measurement of contributions of diffractive processes to forward photon spectra in pp collisions at $\sqrt{s}$ = 13 TeV*, *ATLAS-CONF-2017-075* (2017) .

[7] Q.-D. Zhou, Y. Itow, H. Menjo and T. Sako, *Monte Carlo study of particle production in diffractive proton–proton collisions at $\sqrt{s}$ = 13 TeV with the very forward detector combined with central information*, *The European Physical Journal C* **77** (2017) 212.

[8] O. Adriani et al., *Measurement of forward photon production cross-section in proton–proton collisions at $\sqrt{s}$ = 13 TeV with the LHCf detector*, *Physics Letters B* **780** (2018) 233.